MICROSCOPIC CLUSTER MODEL FOR THE DESCRIPTION OF (^{18}O,^{16}O) TWO-NEUTRON TRANSFER REACTIONS*

D. Carbone[a], J.L. Ferreira[b], F. Cappuzzello[a,c], J. Lubian[b]
C. Agodi[a], M. Cavallaro[a], A. Foti[c,d], A. Gargano[e], S.M. Lenzi[f,g]
R. Linares[b], G. Santagati[a]

[a]INFN — Laboratori Nazionali del Sud, Catania, Italy
[b]Instituto de Fisica, Universidade Federal Fluminense, Niteroi, RJ, Brazil
[c]Dipartimento di Fisica e Astronomia, Università degli Studi di Catania, Italy
[d]INFN — Sezione di Catania, Catania, Italy
[e]INFN — Sezione di Napoli, Napoli, Italy
[f]Dipartimento di Fisica e Astronomia, Università di Padova, Padova, Italy
[g]INFN — Sezione di Padova, Padova, Italy

(Received December 28, 2017)

Excitation energy spectra and absolute cross-section angular distributions were measured for the ^{13}C(^{18}O,^{16}O)^{15}C two-neutron transfer reaction at 84 MeV incident energy. Exact finite-range coupled reaction channel calculations are used to analyse the data considering both the direct two-neutron transfer and the two-step sequential mechanism. For the direct calculations, two approaches are discussed: the extreme cluster and the newly introduced microscopic cluster. The latter makes use of spectroscopic amplitudes in the centre-of-mass reference frame, derived from shell-model calculations. The results describe well the experimental cross sections.

DOI:10.5506/APhysPolB.49.373

1. Introduction

Direct two-nucleon transfer reactions play an important role in the study of specific features of the atomic nucleus and indeed they were extensively explored [1–5] to study, for example, pairing correlations. Among these, heavy-ion direct transfer reactions at energies close to the Coulomb barrier are useful tools to obtain precise spectroscopic information. In this context, a wide range of systems was explored by heavy-ion induced one- and two-neutron transfer reactions at INFN-LNS (Italy), specifically using

* Presented at the XXXV Mazurian Lakes Conference on Physics, Piaski, Poland, September 3–9, 2017.

the (^{18}O,^{17}O) and (^{18}O,^{16}O) reactions. The MAGNEX spectrometer [6] was used to detect the ejectiles. Its large acceptance and high resolution allowed to obtain high-quality energy spectra up to the region above the two-neutron separation energy in the residual nucleus [7–9]. New phenomena were observed, *e.g.* the dominance of the direct one-step transfer of the two neutrons [10] and the presence of the first experimental signature of the Giant Pairing Vibration [11, 12] at high excitation energy in the ^{14}C and ^{15}C spectra. The analysis of the broad structures in the ^{15}C spectrum at high excitation energy was presented in Ref. [13] and the neutron decay of these structures was investigated in Ref. [14], exploiting the use of the EDEN array coupled to the spectrometer [15, 16]. Moreover, it was demonstrated in several works that the (^{18}O,^{16}O) two-neutron transfer reaction can be used for quantitative spectroscopic studies of pair configurations in nuclear states [19–23]. A good description of the reaction mechanisms involved in multi-nucleon transfer reactions is important also to go deep inside the dynamics of more complex processes such as double charge-exchange reactions, which are of interest for obtaining information about the nuclear matrix elements involved in neutrino-less double beta decay [24, 25].

A complete theoretical treatment of the transfer process should contain a description of three terms: the one-step channel with the inclusion of all possible inelastic excitations of the target, projectile, ejectile or residual nucleus; the sequential channel, with the inclusion of intermediate partitions and the non-orthogonal term derived from the limited model space used in actual calculations. As long as heavy ions are concerned, it is necessary to include explicitly the inelastic excitations of the involved nuclei using the coupled-channels approach [26–28]. A complete two-step Coupled Reaction Channel (CRC) approach was employed to study ^{8}He$(p,t)^{6}$He and ^{6}He$(p,t)^{4}$He two-neutron transfer reactions in Refs. [17, 18].

In Ref. [19], the experimental absolute cross sections of the one- and two-neutron transfer reactions induced by an ^{18}O beam on a ^{12}C target were reproduced without any scaling factor by means of Exact Finite Range (EFR) CRC calculations. Two approaches were used: the extreme cluster model and the independent coordinate scheme. The description of these approaches can be found in Refs. [29] and [30], respectively. The same framework was recently applied to describe the absolute cross-section angular distributions of the states populated by the ^{13}C(^{18}O,^{16}O) reaction [21]. A new approach consisting in a fully microscopic cluster calculation is introduced, performed by using the two-neutron spectroscopic amplitudes calculated in the shell-model framework. This new approach can be more extensively used with respect to the extreme cluster model to evaluate the presence of cluster components in the wave functions involved. In this paper, the role of the different partial waves in the microscopic calculation is discussed for some

transitions in ^{15}C nucleus. In particular, the case of the state at 0.74 MeV is analysed, which displays some peculiar features. For this state, also two-step CRC calculations are performed to investigate the role of single-particle components in the wave function.

2. Experimental setup and results

The experiment was performed at the INFN-LNS laboratory using an $^{18}O^{6+}$ beam at 84 MeV incident energy on a thin ^{13}C target. The same measurement was also done on ^{12}C target to estimate the background coming from the ^{12}C impurities in the ^{13}C target. The MAGNEX spectrometer was used to detect the ejectiles [6]. The particle identification and the data reduction technique are the same as described in detail in Refs. [12, 31]. An example of the obtained energy spectra for the ^{15}C nucleus is shown in Fig. 1, in which the ^{14}C background spectrum coming from the ^{12}C impurities in the ^{13}C target is superimposed, after normalization. The strongest bound and resonant states appearing in the spectrum of the ^{15}C nucleus are almost the same that were strongly populated in the (t, p) reactions on ^{13}C [32]. In particular, below the one-neutron separation energy ($S_n = 1.218$ MeV), only two ^{15}C bound states are identified, *i.e.* the ground ($J_\pi = 1/2^+$) and the $5/2^+$ state at $E_x = 0.74$ MeV, that are characterized by a dominant single-particle configuration [33]. In the region between S$_n$ and the two-neutron separation energy ($S_{2n} = 9.39$ MeV), narrow resonances at $E_x = 3.103\,(1/2^-)$,

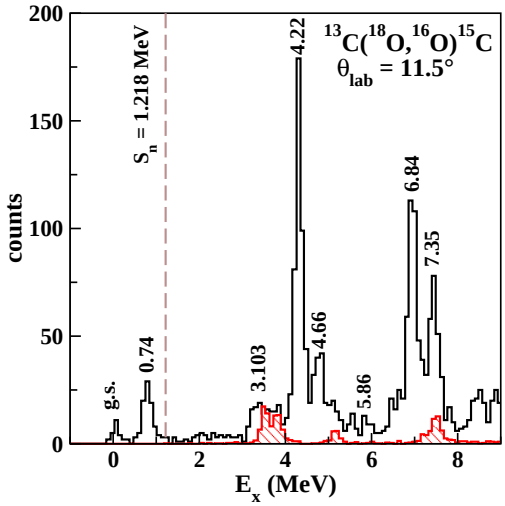

Fig. 1. (Colour on-line) Excitation energy spectrum of the ^{13}C(^{18}O,^{16}O)^{15}C reaction for $10° < \theta_{\rm lab} < 11°$. The hatched (red) area corresponds to the background that comes from ^{12}C impurities in the target. The value of the one-neutron emission threshold is also indicated with the dashed line ($S_n = 1.218$ MeV).

4.22 ($5/2^-$), 4.66 ($3/2^-$), 6.84 ($9/2^-$, $7/2^-$), 7.35 ($9/2^-$, $7/2^-$) MeV are populated. All of these states are indicated to consist mainly of $2p$–$1h$ configurations (with respect to the $^{14}C_{gs}$ vacuum state) [32]. Resonances with a single-particle configuration of a $^{14}C_{gs}+1n$ [34] are very weakly populated in the present reaction. Examples of the obtained absolute cross-section angular distributions for the ground state and the first excited state at 0.74 MeV are shown in Figs. 2 and 3.

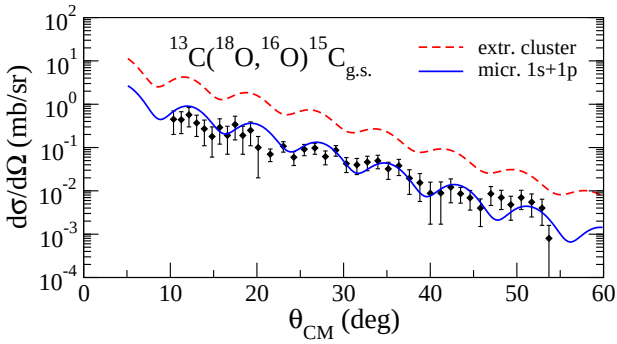

Fig. 2. (Colour on-line) Experimental cross-section angular distributions for the ground state in ^{15}C. Theoretical calculations: extreme cluster calculations (dashed/red line) and microscopic cluster model calculations including $1s + 1p$ waves (solid/blue line).

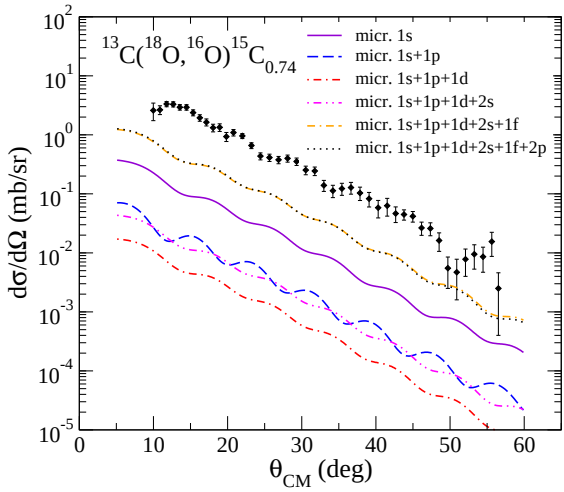

Fig. 3. (Colour-online) Experimental cross-section angular distributions for the state at 0.74 MeV in ^{15}C. Microscopic cluster model calculations including: $1s$ (solid/violet line); $1s+1p$ waves (dashed/blue line); $1s+1p+1d$ (dash-dotted/red line); $1s+1p+1d+2s$ (dash-double-dotted/magenta line); $1s+1p+1d+2s+1f$ (double-dashed-dotted/orange line); $1s+1p+1d+2s+1f+2p$ (dotted/black line).

3. Theoretical analysis

Exact finite-range coupled reaction channel (CRC) calculations were performed to describe the cross section, using the FRESCO code [35], with the same ingredients as in Ref. [19]. Firstly, a direct, simultaneous transfer of the two particles was considered. The two-particle wave functions for the one-step two-neutron transfer mechanism were obtained considering two different schemes: *(i)* the extreme cluster model, in which the relative motion between the two transferred neutrons is frozen and separated from the core, and the two neutrons are coupled antiparallel to an intrinsic angular momentum $S = 0$, with spectroscopic amplitudes for both target and projectile set to 1.0 and *(ii)* the microscopic cluster model, which was introduced in Ref. [21]. The ^{12}C is assumed as a closed core and the model space includes the $1p_{1/2}$, $1d_{5/2}$, $2s_{1/2}$ orbits. The effective phenomenological ZBM interaction [36] was used. When a cluster model is used, the parameters relevant for the definition of the wave function are the principal quantum number N and the orbital angular momentum L relative to the core. These parameters are obtained from the conservation of the total number of quanta in the transformation of the wave function of two independent neutrons in orbits $(n_i,\ l_i)$ $(i = 1, 2)$ into a cluster with internal state (n, l) [31]: $2(n_1 - 1) + l_1 + 2(n_2 - 1) + l_2 = 2(N - 1) + L + 2(n - 1) + l$. In the extreme cluster model hypothesis, we consider $n = 1$ and $l = 0$ so that the cluster is in a $1s$ internal state. The spectroscopic amplitudes for both target and projectile were set to 1.0. The resulting differential cross section using the extreme cluster hypothesis for the ground state is shown in Fig. 2. Using this extreme approximation, the calculations give in this case a cross section larger than the experimental one. The main reason for this overestimation may lie in the approximation that the two neutrons are coupled to the total spin $S = 0$ with 100% of probability.

A natural way to go beyond the assumptions of the extreme cluster model is to introduce both parallel and antiparallel couplings for the two neutrons. Realistic spectroscopic amplitudes are required for all possible combinations of single-particle configurations in this enlarged space that can be derived from shell-model calculations. To achieve this goal, we made use of transformations from individual (j–j coupling) to relative and centre-of-mass coordinates (LS coupling) for the harmonic-oscillator wave functions of the two-particle system [21], using the Moshinsky brackets [37]. This approach is what we call microscopic cluster calculations. We performed microscopic cluster calculations considering that the cluster relative motion state is represented by $n = 1$ and $l = 0$ quantum numbers, *i.e.* the cluster is in the $1s$ intrinsic state, and $n = 1$ and $l = 1$ ($1p$ intrinsic state). The

results are shown in Fig. 2 for the ground state. We see that the results of $(1s + 1p)$ microscopic cluster calculations are in rather good agreement with the experimental angular distributions, and this is true also for the transitions at 3.103, 4.22 and 4.66 MeV.

3.1. Analysis of the 0.74 MeV state

The behaviour of the state at 0.74 MeV is very different from the others. Passing from the microscopic calculation with only the $1s$ wave to the $(1s + 1p)$ waves, the obtained cross sections decrease. This is probably due to a destructive interference between the $1s$ and the $1p$ waves. We tried to add more waves in this case, in particular the $1d$ ($n = 1$ and $l = 2$), $2s$ ($n = 2$ and $l = 0$), $1f$ ($n = 1$ and $l = 3$) and $2p$ ($n = 2$ and $l = 1$). The results are shown in Fig. 3. The inclusion of the $1d$ wave decreased even more the calculated cross section, then with adding step by step the other waves the results start to increase, up to a saturation for the $(1s + 1p + 1d + 2s + 1f)$ and $(1s + 1p + 1d + 2s + 1f + 2p)$ cases. The only wave which contributes a lot to the calculated cross section is the $1f$. This corresponds to a configuration of $|^{13}\mathrm{C}_{\mathrm{gs}}(1/2^-)\rangle$ coupled with two neutrons with $l = 3$, which gives the $|^{15}\mathrm{C}_{0.74}(5/2^+)\rangle$ state. The discrepancy still found between the calculations and the data is probably due to the dominant single-particle configuration of this state, built as $|^{15}\mathrm{C}_{0.74}(5/2^+)\rangle = |^{14}\mathrm{C}_{\mathrm{gs}}(0^+)\rangle \bigotimes (1d_{5/2})^{\nu}$ with spectroscopic factor close to 1 [33]. For this reason, the cluster model adopted for these calculations is not the suitable approach for such kind of states, which do not present strong cluster components in the wave function.

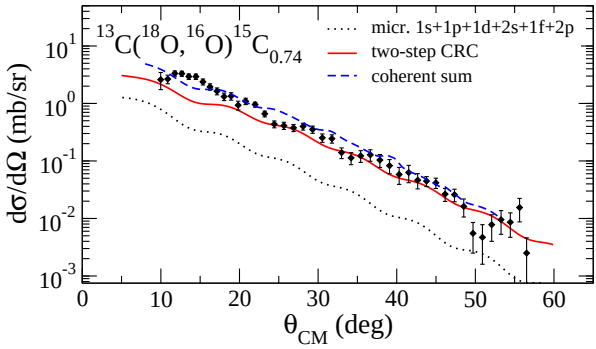

Fig. 4. (Colour on-line) Experimental cross section angular distributions for the state at 0.74 MeV in ^{15}C. Microscopic cluster model calculations including $1s + 1p + 1d + 2s + 1f + 2p$ (dotted/black line), two-step CRC calculations (solid/red line) and coherent sum between them (dashed/blue line).

Two-step sequential CRC calculations, introducing the $^{17}O + {}^{14}C$ intermediate partition, were also performed to improve the results for the transition to this state. The coupling scheme is the same reported in Ref. [21]. The obtained results are in better agreement with the data with respect to the microscopic cluster model calculations, as visible in Fig. 4. This confirms the importance of single-particle components for this state. Following the technique described in Ref. [19], we performed also the coherent sum of the sequential CRC cross sections and the $1s + 1p + 1d + 1f + 2p$ microscopic cluster and the result is shown in Fig. 4. The interference between the direct and sequential mechanisms provides a little improvement in the description of the experimental data.

4. Conclusions

We reported the spectrum and cross-section angular distributions obtained for the two-neutron transfer reaction $^{13}C(^{18}O,^{16}O)^{15}C$ at 84 MeV incident energy. The experimental cross sections for the population of the states in ^{15}C are reasonably well-described by one-step CRC calculations with no need for any "unhappiness" factor. The new microscopic cluster model allows to describe rather well the experimental cross sections for the transitions in which cluster components are important. For the 0.74 MeV state, which contains strong single-particle components, it was necessary to add the sequential two-step mechanism to describe the cross section.

This project has received funding from the European Research Council (ERC) under the European Union's Horizon 2020 research and innovation programme (grant agreement No. 714625).

REFERENCES

[1] S. Mordechai *et al.*, *Nucl. Phys. A* **301**, 463 (1978).
[2] P. Guazzoni *et al.*, *Phys. Rev. C* **83**, 044614 (2011).
[3] P. Guazzoni *et al.*, *Phys. Rev. C* **69**, 024619 (2004).
[4] G. Potel *et al.*, *Phys. Rev. Lett.* **107**, 092501 (2011).
[5] G. Potel *et al.*, *Phys. Rev. Lett.* **105**, 172502 (2010).
[6] F. Cappuzzello *et al.*, *Eur. Phys. J. A* **52**, 167 (2016).
[7] D. Carbone *et al.*, *Phys. Rev. C* **90**, 064621 (2014).
[8] D. Nicolosi *et al.*, *Acta Phys. Pol. B* **44**, 657 (2013).
[9] D. Carbone *et al.*, *Acta Phys. Pol. B* **45**, 431 (2014).
[10] D. Carbone *et al.*, *J. Phys.: Conf. Ser.* **312**, 082016 (2011).

[11] F. Cappuzzello *et al.*, *Nat. Commun.* **6**, 6743 (2015).
[12] D. Carbone, *Eur. Phys. J. Plus* **130**, 143 (2015).
[13] F. Cappuzzello *et al.*, *Phys. Lett. B* **711**, 347 (2012).
[14] M. Cavallaro *et al.*, *Phys. Rev. C* **93**, 064323 (2016).
[15] H. Laurent *et al.*, *Nucl. Instrum. Methods Phys. Res. A* **326**, 517 (1993).
[16] M. Cavallaro *et al.*, *Nucl. Instrum. Methods Phys. Res. A* **700**, 65 (2013).
[17] N. Keeley *et al.*, *Phys. Lett. B* **646**, 222 (2007).
[18] K. Rusek, L. Giot, P. Roussel-Chomaz, *Eur. Phys. J. A* **32**, 159 (2007).
[19] M. Cavallaro *et al.*, *Phys. Rev. C* **88**, 054601 (2013).
[20] M.J. Ermamatov *et al.*, *Phys. Rev. C* **94**, 024610 (2016).
[21] D. Carbone *et al.*, *Phys. Rev. C* **95**, 034603 (2017).
[22] M.J. Ermamatov *et al.*, *Phys. Rev. C* **96**, 044603 (2017).
[23] B. Paes *et al.*, *Phys. Rev. C* **96**, 044612 (2017).
[24] F. Cappuzzello *et al.*, *Eur. Phys. J. A* **51**, 145 (2015).
[25] F. Cappuzzello *et al.*, *J. Phys.: Conf. Ser.* **630**, 012018 (2015).
[26] P.D. Bond *et al.*, *Phys. Rev. C* **16**, 177 (1977).
[27] M.C. Lemaire, K.S. Low, *Phys. Rev. C* **16**, 183 (1977).
[28] D. Pereira *et al.*, *Phys. Lett. B* **710**, 426 (2012).
[29] G.R. Satchler, *Direct Nuclear Reactions*, Oxford University Press, 1983.
[30] I.J. Thompson, *Comput. Phys. Rep.* **7**, 167 (1988).
[31] F. Cappuzzello *et al.*, *Nucl. Instrum. Methods Phys. Res. A* **763**, 314 (2014).
[32] S. Truong, H.T. Fortune, *Phys. Rev. C* **28**, 977 (1983).
[33] G. Murillo, S. Sen, S.E. Darden, *Nucl. Phys. A* **579**, 125 (1994).
[34] J.D. Goss *et al.*, *Phys. Rev. C* **8**, 514 (1973).
[35] J.I. Thompson, `http://www.fresco.org.uk/`
[36] A.P. Zuker, B. Buck, J.B. McGrory, *Phys. Rev. Lett.* **21**, 39 (1968).
[37] M. Moshinsky, *Nucl. Phys.* **13**, 104 (1959).